Limited and strain-specific transcriptional and growth responses to acquisition of a multidrug resistance plasmid in genetically diverse *Escherichia coli* lineages

Steven J. Dunn*[1], Laura Carrilero*[2], Michael Brockhurst[2], Alan McNally[1]

*Joint first authors contributed equally

[1]Institute of Microbiology and Infection, College of Medical and Dental Science, University of Birmingham, Birmingham B15 2TT

[2]Division of Evolution and Genomic Sciences, School of Biological Sciences, University of Manchester, Manchester M13 9PT

Running title: Transcriptional response to MDR plasmids in *E. coli*

Abstract

Multi-drug resistant (MDR) *Escherichia coli* are a major global threat to human health, wherein multi-drug resistance is primarily spread by MDR plasmid acquisition. MDR plasmids are not widely distributed across the entire *E. coli* species, but instead are concentrated in a small number of clones. Here, we test if diverse *E. coli* strains vary in their ability to acquire and maintain MDR plasmids, and if this relates to their transcriptional response following plasmid acquisition. We used strains from across the diversity of *E. coli*, including the common MDR lineage ST131, and the IncF plasmid, pLL35, encoding multiple antibiotic resistance genes. Strains varied in their ability to acquire pLL35 by conjugation, but all were able to stably maintain the plasmid. The effects of pLL35 acquisition on cefotaxime resistance and growth also varied among strains, with growth responses ranging from a small decrease to a small increase in growth of the plasmid-carrier relative to the parental strain. Transcriptional responses to pLL35 acquisition were limited in scale and highly strain specific. We observed significant transcriptional responses at the operon or regulon level, possibly due to stress responses or interactions with resident MGEs. Subtle transcriptional responses consistent across all strains were observed affecting functions, such as anaerobic metabolism, previously shown to be under negative frequency dependent selection in MDR *E. coli*. Overall there was no correlation between the magnitude of the transcriptional and growth responses across strains. Together these data suggest that fitness costs arising from transcriptional disruption are unlikely to act as a barrier to MDR plasmid dissemination in *E. coli*.

38 **Importance**

39 Plasmids play a key role in bacterial evolution by transferring niche adaptive functions
40 between lineages, including driving the spread of antibiotic resistance genes. Fitness
41 costs of plasmid acquisition arising from the disruption of cellular processes could limit
42 the spread of multidrug resistance plasmids. However, the impacts of plasmid
43 acquisition are typically measured in lab-adapted strains rather than in more
44 ecologically relevant natural isolates. Using a clinical multidrug resistance plasmid and
45 a diverse collection of *E. coli* strains isolated from clinical infections and natural
46 environments, we show that plasmid acquisition had only limited and highly strain-
47 specific effects on bacterial growth and transcription. These findings suggest that
48 fitness costs arising from transcriptional disruption are unlikely to act as a barrier to
49 plasmid transmission in natural populations of *E. coli*.

50

51 **Introduction**

52 Multi-drug resistant (MDR) *Escherichia coli* present a global public health risk and are
53 listed by the World Health Organisation as a priority pathogen. The incidence of MDR
54 *E. coli* as aetiological agents of human disease has steadily increased since the turn
55 of the century (Mathers et al., 2015). Initially this was due to the emergence of *E. coli*
56 clones carrying plasmids containing extended spectrum beta-lactamase (ESBL)
57 genes conferring resistance to third generation cephalosporins (Mathers et al., 2015).
58 This emergence mirrored the rise in the incidence of *E. coli* as the causative agent of
59 bloodstream infections world-wide, primarily due to the rapid global dissemination of
60 MDR clones (Banerjee & Johnson, 2014; Mathers et al., 2015). This was followed by
61 the emergence of clones carrying plasmids containing carbapenemase enzyme
62 genes, conferring strains resistance to all antimicrobial classes with the exception of
63 colistin (Peirano et al., 2011; Wu et al., 2019).

64

65 The emergence of MDR *E. coli* has not occurred evenly across the species. Rather
66 MDR plasmid carriage is concentrated in a number of clones associated with extra-
67 intestinal infections, whilst it is rarely seen in clones causing intestinal infectious
68 disease or in exclusively commensal lineages (Dunn et al., 2019). ESBL plasmid
69 carriage is most commonly seen in low-diversity clones of lineages such as ST131,
70 ST648, and ST410 (Dunn et al., 2019), with ST131 representing the most common
71 cause of MDR *E. coli* bloodstream and urine infections in the developed world
72 (Banerjee & Johnson, 2014). Carriage of carbapenemase plasmids is also
73 concentrated in low-diversity clones of lineages such as ST167 and ST410, both of
74 which belong to the Phylogroup A clade of *E. coli* which are generally devoid of most
75 common *E. coli* virulence factors (Feng et al., 2019; Wu et al., 2019; Zong et al., 2018).

Comparison of the genomes of MDR plasmid carrying clones with the lineages that those clones emerged from shows striking similarity in key steps in their evolution. All show rapid clonal expansion of MDR plasmid carrying strains which are globally distributed in a matter of years (Feng et al., 2019; Petty et al., 2014; Zong et al., 2018). The MDR clones also carry clone specific alleles of key genes encoding traits involved in human colonisation, such as adhesins and iron acquisition (Feng et al., 2019; McNally et al., 2019; Zong et al., 2018). Comprehensive analysis of ST131 MDR clade C showed it differed from the drug susceptible clade A and B of the lineage in a number of unique alleles of genes involved in colonisation as well as anaerobic metabolism genes (McNally et al., 2019). MDR clones also contain unique intergenic-sequence alleles, which correlate with plasmids carried by strains (McNally et al., 2016)(Feng et al., 2019; Zong et al., 2018).

As well as the biosynthetic burden associated with replicating, transcribing and translating the new genetic material, plasmid acquisition often disrupts cellular homeostasis. For example, large-scale changes to regulation of chromosomal genes have been observed following plasmid acquisition in a range of bacterial hosts (Harrison et al., 2015; Millan et al., 2015; San Millan et al., 2018), which can be negated by compensatory mutations to regulators. The shared genetic traits of MDR clones of *E. coli* including regulatory sequences together with the uneven distribution of MDR plasmids, suggests that some lineages of *E. coli* may be better preadapted to the acquisition and stable integration of MDR plasmids than others, potentially suffering less cellular disruption (Dunn et al., 2019; McNally et al., 2016). However, data comparing the transcriptional and phenotypic responses of diverse *E. coli* strains to MDR plasmid acquisition are lacking.

101 We tested the transcriptional response to acquisition of an ESBL plasmid encoding
102 CTX-M-15 and TEM-112 in eight genetically diverse *E. coli* strains, including
103 environmental *E. coli* isolates from lineages in which MDR plasmids have never been
104 reported, and strains from clade A, B and C of *E. coli* ST131, wherein clade C is most
105 frequently associated with MDR plasmid acquisition. Strains varied in the rate of ESBL
106 plasmid acquisition by conjugation from *K. pneumoniae* and the degree of cefotaxime
107 resistance conferred by the plasmid but not in stability of the plasmid once acquired.
108 ESBL plasmid carriers showed variations in growth relative to plasmid free cells
109 ranging from impaired to enhanced relative growth of ESBL plasmid carriers. Plasmid
110 transcription did not vary significantly among host strains, but we observed strain
111 specific differences in chromosomal gene expression caused by plasmid acquisition.
112 We observed no correlation between the degree of transcriptional disruption caused
113 by plasmid acquisition and the relative growth of ESBL plasmid carriers.
114
115 **Materials and Methods**
116
117 **Bacterial strains and plasmids**
118 A total of 8 *E. coli* strains were selected for use in this study, representing sequence
119 types 131 (clades A, B, and C), 394, and 1122 (Table S1). All strains were screened
120 to ensure that they did not contain any existing MDR plasmids. This study used
121 plasmid donor strain LL35 (a *Klebsiella pneumoniae* isolate belonging to ST-45) which
122 contains pLL35, a 106 kb incFII(K)-9 plasmid with a complete conjugative transfer
123 machinery, and a complex antibiotic resistance region (Figure S1). The resistance
124 region in pLL35 is comprised of multiple translocatable genetic elements. It contains
125 several complete antibiotic resistance genes, conferring resistance to cephalosporins

126 and beta-lactams (*blaCTX-M-15*, *blaTEM-112*), aminoglycosides (*aacA4, aacC2,*
127 *aadA1*) and quinolones (*qnrS1*). This region also contains OXA-9, however this gene
128 is truncated due to a premature stop codon. The antibiotic resistance region is
129 potentially mobilizable, due to an ISEcp1 insertion sequence. pLL35 also encodes two
130 separate toxin/antitoxin systems (*higAB*, *ccdAB*).
131
132 **Plasmid conjugation**
133 Twelve independent conjugation assays were performed for each strain. A single
134 colony from overnight growth on nutrient agar was inoculated into 5 ml of nutrient broth
135 (Oxoid, UK). This was incubated at 37˚C for 2 hours with shaking (180 rpm). Cultures
136 were mixed at a ratio of 1:3 donor to recipient and 50 µl were used to inoculate 6 ml
137 of BHI. Six replicates were incubated as static cultures at 37˚C for 24 hours, and six
138 replicates were incubated as shaken cultures at 37˚C for 24 hours at 180 rpm.
139
140 The conjugation mix was plated onto UTI Chromagar (Sigma Aldrich, UK)
141 supplemented with 4 µg/ml of cefotaxime and incubated at 37˚C overnight. Colonies
142 that produced a phenotype indicative of *E. coli* were further subcultured onto UTI
143 Chromagar with 4 µg/ml of cefotaxime in order to check the resistance profile, and to
144 ensure there was sufficient pure growth to store for subsequent use. One of these
145 replicates was used to quantify differential gene expression and is subsequently
146 referred to as the transconjugant. Whole genome sequencing (WGS) data was also
147 generated for three additional replicates from the conjugation assays, which are
148 referred to as the transconjugant replicates.
149

150 In the generation of conjugated strains, bacteria were sub-cultured a total of 5 times.
151 In order to account for any basal adaptation to the lab conditions, and to control for
152 any variation generated by variables extraneous to the plasmid conjugation, the
153 parental recipient strains were also run through the conjugation protocol with a plasmid
154 free *Klebsiella* strain Ecl8 (Buckner et al., 2018). These triplicate samples were also
155 sequenced and are referred to as the control replicates.
156
157 **Genome sequencing**
158 Whole genome sequencing was performed on the ancestral, transconjugant, control
159 replicates and transconjugant replicate strains. The ancestral and transconjugant lines
160 were sequenced by both Illumina and Oxford Nanopore based technologies. Illumina
161 sequencing was provided by MicrobesNG (http://www.microbesng.com). Illumina
162 genome sequence reads were assessed for quality using FastQC (V 0.11.9), and
163 subsequently trimmed using Trimmomatic (V 0.3)14 with a sliding window quality of
164 Q15 and length of 20 base pairs. Kraken (V 2) was used to confirm species ID and
165 check for potential contaminants.
166
167 Long read sequencing was performed on DNA extracted using a phenol/chloroform
168 method. DNA was quantified using the Qubit 4.0 and a broad range dsDNA kit
169 (ThermoFisher, UK). Libraries were prepared using the SQK-LSK109 sequencing kit,
170 and EXP-NBD104 expansion set. The libraries were then sequenced on a MinION rev
171 4.1D using a R9.1 flowcell over 48 hours (Oxford Nanopore Technologies,
172 UK).MinION data was basecalled using GPU-accelerated Guppy (V 3.1.5+781ed57)
173 in high accuracy mode. Adapters were confirmed and removed using Porechop (V
174 0.2.3_seqan2.1.1). Reads that had differential demultiplexing via Guppy and

175 Porechop were discarded, leaving only reads for which both programs had reached a
176 consensus. Chimeric reads were discarded using Unicycler's Scrub module (V 0.4.7).
177 Finally, reads were filtered using FiltLong (V 0.2.0), with parameters based on read
178 length and quality distributions generated by NanoPlot (V 1.24.0), removing relatively
179 short or low-quality reads (e.g. lower 10% of the distribution).
180
181 Circularised assemblies were produced using both the long and short read data by
182 Unicycler (V 0.4.7) (Wick et al., 2017). Following assembly, we ran additional rounds
183 of Pilon (V 1.23) until no further changes were found. Assemblies were annotated
184 using Prokka (V 1.13.3) (Seemann, 2014). Structural variants were identified using a
185 combination of Sniffles (V 1.0.12) and Assemblytics (V 1.0). Structural variants were
186 further filtered to high confidence calls by inspecting the BAM file and filtering to
187 discard minor allele variants (AF <0.9). Single nucleotide variants were called against
188 the hybrid assemblies using Snippy (V 4.3.6).
189
190 **Transcriptome sequencing**
191 RNA sequencing was performed on biological triplicates of the ancestral and
192 transconjugant strains. For each replicate, a colony was picked from overnight growth
193 on Nutrient Agar and added to 5 ml of Nutrient Broth (Sigma Aldritch, UK). Cultures
194 were incubated at 37˚C until reaching an OD600 of ~0.6. RNA was extracted using
195 Trizol (ThermoFisher, UK). Following isopropanol precipitation, DNA was digested
196 using Turbo DNAse (Thermofisher, UK) based on the manufacturer's protocol. The
197 final RNA solution was purified using a RNeasy Mini Kit (Qiagen, UK), and quantified
198 using a Qubit with the RNA HS assay kit. The RNA was immediately stored at -80˚C.
199

200 RNA sequencing was performed by the Centre for Genomics Research (Liverpool,
201 UK). The RNA integrity number and library insert size were verified using the Agilent
202 RNA 6000 Pico Kit and Bioanalyzer platform (Agilent, USA). The RiboZero (Illumina,
203 USA) kit was used to deplete rRNA, and dual indexed libraries were prepared using
204 the NEBNext Ultra Directional RNA sequencing kit (New England Biolabs, USA).
205 Libraries were sequenced on a HiSeq 4000 (Illumina, USA) configured to 2 x 150 bp
206 cycles. In order to obtain at least 10 million reads per sample, the sequencing run was
207 distributed across three lanes.
208
209 Kallisto (v 0.46.0) was used to quantify differential gene expression, with the high-
210 quality hybrid *de novo* assemblies of parental strains used as a reference. Input files
211 were prepared using Prokka (v 1.13.3) for annotation, genbank_to_kallisto.py
212 (https://github.com/AnnaSyme/genbank_to_kallisto.py) to convert the annotation files
213 for use with Kallisto, and GNU-Parallel (v 20180922) for job parallelisation. Differential
214 gene expression was analysed using Voom/Limma in Degust (V 3.20), with further
215 processing of the resulting differential counts in R (V 3.5.3). UPGMA clustering was
216 performed using DendroUPGMA (http://genomes.urv.cat/UPGMA/). Functional
217 categories were assigned to genes using eggnog-mapper (V 2).
218
219 **Plasmid persistence**
220 To determine the persistence of the plasmid over time, 4 replicate cultures of each
221 plasmid-containing strain were propagated by daily serial transfer in nutrient broth
222 (NB) microcosms (6 ml of NB in a 30 ml glass universal) for 16 days. 1% of each
223 culture was transferred to fresh media every 24 hours. Populations were plated out
224 onto nutrient agar ± 4μg/ml of cefotaxime at days 0, 1, 2, 4, 7, 10, 13 and 16.

225 **Growth curves and phenotypic profiling**

226 Minimum inhibitory concentration (MIC) assays for the ancestral and transconjugant
227 strains were conducted according to the CLSI guidelines (CLSI, 2012), using nutrient
228 broth and cefotaxime. Briefly, assays were performed in 96 well plates at final
229 cefotaxime concentrations of 0.25, 0.5, 0.75, 1, 1.25, 1.5, 1.75, and thereafter two-fold
230 increases from 2 to 2,048 µg/ml.

231

232 Growth kinetics for both plasmid-free and plasmid-containing strains were measured
233 using cultures grown in 200 µl nutrient broth per well in a 96 well plate using an
234 automated absorbance plate reader (Tecan Spark 10). Wells were inoculated using
235 the same procedure described above. Plates were incubated at 37 °C for 39 hours
236 and the optical density of each well was measured every 30 minutes at 600 nm, plates
237 were shaken for 5s (orbital shaking, movement amplitude 3mm, 180 rpm) and allowed
238 to settle for 50s prior to each reading. A humidity cassette was used to minimise
239 evaporation of the samples.

240

241 **Data availability**

242 Sequence data is available under bioproject PRJNA667580, and individual SRA
243 accessions are provided in Table S1.

244

245 **Results**

246

247 ***E. coli* strains varied in conjugational uptake of an ESBL plasmid**

248 For most strains, the conjugation rate from *K. pneumoniae* was higher in static than in
249 shaken culture. Indeed, for several strains we detected no transconjugants from

250 shaken cultures in any of the replicates (e.g., F022 and F047 – ST131 clade A and C,
251 respectively), and only three strains consistently acquired the plasmid in both shaken
252 and static conditions (i.e., F037, F048, F054 – all ST131 clade B/C – Figure S1). Due
253 to the high number of missing replicates in shaken cultures, we were only able to
254 analyse variation across all strains in the conjugation rates estimated from static
255 cultures. In static cultures, strains varied in their ability to acquire the plasmid by
256 conjugation from *K. pneumoniae* (Figure S2; ANOVA, strain effect, $F_{7,36}$ = 19.23 P =
257 2.06e-10). Once acquired, however, the plasmid was stably maintained over time by
258 all strains (Figure S3; Wilcoxon test comparing population density averaged over time
259 on media with or without cefotaxime, all strains, P > 0.05).
260

261 **Strain-specific effects of ESBL plasmid carriage on resistance and bacterial**
262 **growth kinetics**

263 Plasmid acquisition increased resistance to cefotaxime but the level of resistance
264 conferred by the plasmid varied by strain (Figure 1; ANOVA, strain by plasmid
265 interaction, $F_{7, 32}$ = 2.968, P = 0.0163). Specifically, in strains F037, F047 and F054
266 the plasmid provided lower levels of cefotaxime resistance than in plasmid bearers of
267 the other strains.
268

269 Parental strains varied in their growth parameters (lag time, ANOVA, $F_{7, 32}$ = 5.358, P
270 = 0.000394; maximum growth rate, ANOVA, $F_{7, 32}$ = 6.3, P = 0.000108; saturation
271 density, ANOVA, $F_{7, 32}$ = 18.48, P = 0.00000000136; integral of the growth curve,
272 Kruskal-Wallis X^2_7 = 31.759, P = 0.000045). To control for this variation in baseline
273 growth among the strains, we normalised growth parameters per plasmid-carrying
274 strain by its corresponding parental strain. This gave estimates of relative growth

275 parameters, and thus of the impact of plasmid acquisition upon the growth of each
276 strain (i.e., a value of 1 would indicate no effect on growth of plasmid acquisition;
277 Figure 2). Strains varied in their relative maximum growth rate (ANOVA, $F_{7, 32} = 5.742$,
278 $P = 0.00023$), relative saturation density (Kruskal-Wallis $\chi^2_7 = 24.102$, $P = 0.001093$),
279 and relative integral of the growth curve (ANOVA, $F_{7, 32} = 8.998$, $P = 0.00000424$), but
280 not in their relative lag time (Kruskal-Wallis $\chi^2_7 = 10.264$, $P = 0.1741$). The clearest
281 impacts of plasmid acquisition on growth were apparent for the relative integral of the
282 growth curve (Figure 2), which is a useful measure of the overall effect of plasmid
283 acquisition on growth (Wright et al., 2018): The integral of the growth curve was
284 reduced by plasmid carriage in the strains GU15 and F047 (one-sample t-test of
285 relative integral against 1; GU15, $t = 3.6933$, $df = 4$, $P = 0.021$; F047, $t = 4.1762$, $P =$
286 0.014) but was increased in the strains F022 and F037 (one-sample t-test of relative
287 integral against 1; F022, $t = 7.0987$ $df = 4$ $P = 0.0021$; F037, $t = 5.0836$, $P = 0.0071$).
288 Thus, acquiring the ESBL plasmid had variable effects upon growth across the strains
289 causing both increased and decreased growth, whilst having a negligible impact upon
290 the growth of half of the strains tested.
291
292 Following the masking of any variants that occurred in the ancestral or control
293 sequence data, ESBL plasmid carriers contained very few SNPs, with the majority of
294 isolates containing no SNPs at all (n=6 out of 8). The position of detected SNPs was
295 determined, but no clear evidence of parallelism could be established (Table S2). To
296 confirm this limited genomic impact further, we sequenced three additional
297 independently constructed transconjugant replicates. This also revealed a small
298 number of SNPs (0-2 SNPs per replicate), with the majority of sequences containing
299 0 variants (n=16 out of 24).

300

301 **Strain specific transcriptional responses to acquisition of an ESBL plasmid**

302 We next compared the transcriptomes of the pLL35 carrying transconjugants with their
303 parental strain to determine the effect of ESBL plasmid acquisition on host gene
304 expression. Combining differential gene expression analysis from three independent
305 biological replicates showed very little significant transcriptional response in any strain,
306 with the number of significantly 2-fold differentially expressed genes ranging from 22
307 to zero at a false discovery rate (FDR) P-value of < 0.05 and 31 to zero at a FDR P-
308 value of < 0.1 (Figure S3). Volcano plots for the transcriptional impact of ESBL plasmid
309 acquisition per strain show highly strain-specific responses to acquisition of the ESBL
310 plasmid, both in terms of the level of transcriptional response and the genes that were
311 differentially expressed (Figure 3). Strains ELU39, F104 and F037 showed no
312 significant changes in gene expression upon acquisition of the plasmid (at FDR P-
313 value of < 0.05 or < 0.1), strains GU15, F054 and F048 had fewer than 5 genes
314 significantly differentially expressed, and strains F022 and F047 showed between 10
315 and 22 genes significantly differentially expressed (at FDR P-value of < 0.05, Figure
316 S4). There was no correlation between magnitude of transcriptional response and the
317 growth responses observed in the strains (r = -0.6162, P = 0.1038).

318

319 **Functions whose expression was affected by ESBL plasmid acquisition varied**
320 **between strains**

321 We observed differences in the functions whose expression was significantly affected
322 by ESBL plasmid acquisition between the strains. In F022 plasmid-carriers we
323 observed upregulation of the entire class 1, 2 and 3, flagella biosynthesis regulons
324 relative to the plasmid-free parental strain (Chilcott & Hughes, 2000). Further

325 inspection of the genome sequences of the parental and transconjugant F022 strains
326 revealed that this occurred due to an insertion of an IS1 family IS element in *lrhA,* the
327 negative regulator of *flhDC* (Figure 4).
328
329 In F047 the ESBL plasmid caused upregulation of a variety of chromosomal genes,
330 including those involved in various stress responses such as *cpxP* (envelope stress
331 response), *deaD* (low temperature response), *ibpAB* (heat and oxidative stress), and
332 *soxS* (superoxide stress master regulator). This is mirrored in several differentially
333 expressed genes just below the 2 log fold change significance threshold such as *dnaJ,*
334 *degP* and *osmY* (1.81, 1.64 1.59 FC), which are all involved in stress response. The
335 presence of plasmid also led to upregulation of *marR*, the repressor of the *mar*
336 antibiotic resistance and oxidative stress response regulon, though *marA* expression
337 was not significantly affected (1.0 FC, 0.57 FDR). Other functions upregulated by
338 plasmid acquisition included metabolic transport (*mgtA, pstS*) and anaerobic
339 metabolism genes (*glpD*).
340
341 In F048, several co-located hypothetical genes were upregulated, 3 of these were
342 significantly upregulated while the remainder were slightly below the FDR significance
343 threshold. This region was further characterised with Prophage Hunter, showing a
344 putative ~60 Kb prophage. This prophage contains 78 genes and shows 94% identity
345 and 28% coverage with prophage CUS-3. No evidence of phage mobilisation was
346 detected by structural variant analysis, and the read depth at this region (normalised
347 to house-keeping genes) was consistent across both the parental and transconjugant
348 read sets suggesting that the observed upregulation was not due to the presence of
349 additional prophage copies.

350

351 In GU15 the ESBL plasmid led to down regulation of the entire sulfur biosynthesis and
352 transport operons (*cysA* – *cysW*). Significant downregulation was observed in *cysA* at
353 FDR >0.05, and *genes cysHIJKNWU* at FDR >0.1. The rest of the operon were
354 expressed at ranges slightly below the FDR significance threshold.

355

356 **Consistent pattern of low-level transcriptional response to acquisition of the**
357 **ESBL plasmid**

358 Some genes known to be in operons or regulons did not pass significance threshold
359 in our FDR analysis, despite the rest of the operon or regulon doing so. This is due to
360 our use of amalgamated data from three independent biological replicates and strict
361 significance thresholds. We decided to further analyse the expression of all core genes
362 (Figure S5) using a principal component analysis to detect genes that were
363 differentially expressed across our host range (Figure S6). Analysis of this set of genes
364 showed some consistent patterns of differential expression across all strains. A
365 common pattern of upregulation in response to acquisition of the ESBL plasmid was
366 observed for the *cit* operon, *his* operon, the *hya, hyb,* and *hyc* operon, and the *nar* and
367 *ttd* operons and the *gad* loci (Figure 5). Conversely, there was a common pattern of
368 down-regulation in response to acquisition of the ESBL plasmid of the *csg, gat, waa,*
369 *yad,* and *yih* operons across all strains. Functional enrichment analysis of genes in the
370 5th and 95th percentile of these differentially expressed loci confirmed this consistent
371 fine-scale transcriptional response to the plasmid in genes associated with the cell
372 wall, signal transduction, cell motility, energy production and conversion, and
373 carbohydrate transport and metabolism (Figure 5).

374

375 **Discussion**

376 Evidence from experimental evolution studies has provided us with a detailed picture
377 of the impact that acquisition of plasmids and their stable integration into a host cells
378 genetic inventory has on cell fitness (Brockhurst et al., 2019). Much of this fitness
379 impact is driven by changes in transcription in the acquiring cell, both the need to
380 transcribe genes on the plasmid, but also global effects on host cell transcription to
381 offset the impact of carrying the plasmid (Buckner et al., 2018; Harrison et al., 2015;
382 Millan et al., 2015). There are very few of these studies examining the impact of
383 acquisition of multi-drug resistance plasmids on cells from genetically diverse strains
384 (Buckner et al., 2018), with most evidence of adaptations that occur as a result of MDR
385 plasmid acquisition stemming from large comparative population genomics studies
386 (Feng et al., 2019; McNally et al., 2016, 2019). Here we address this by examining the
387 impact of acquisition of an MDR plasmid on *E. coli* from a variety of genetic
388 backgrounds ranging from environmental lineages with no reported MDR plasmid
389 carriage to MDR-plasmid-free clinical isolates from the ST131 lineage most commonly
390 associated with multi-drug resistance in clinical settings.

391

392 Acquisition of the ESBL plasmid varied among strains, although all strains stably
393 maintained the plasmid once they had acquired it, likely due to the presence of two
394 toxin-antitoxin systems on pLL35. Plasmid acquisition had variable effects on growth
395 between strains. Notably, plasmid acquisition was not costly in terms of relative growth
396 for all the strains, with increased growth of plasmid carriers relative to their parentals
397 observed in two strains. This is surprising given that plasmid acquisition has been
398 shown to be associated with fitness costs across a diversity of plasmid-host
399 interactions, although variation in the magnitude of the cost has been described

400 (Bouma & Lenski, 1988; Göttig et al., 2016; Kottara et al., 2018; Nang et al., 2018).
401 However, our data are consistent with those of another recent study that tested the
402 fitness effect of a given plasmid across the range of genetic backgrounds present in a
403 host species. Like ours this study reveal diverse fitness impacts ranging across a
404 continuum from costly to beneficial (Alonso-del Valle et al., 2020). These data highlight
405 that the fitness effects of a plasmid can be highly strain-specific, and thus are likely to
406 arise from specific genetic interactions rather than the generic biosynthetic costs of
407 plasmid maintenance. Interestingly, effects on growth of plasmid acquisition were
408 uncorrelated with the extent of changes in gene expression across the strains,
409 suggesting that greater plasmid-mediated gene dysregulation does not necessarily
410 translate to larger fitness costs.
411
412 Strains varied in the level of cefotaxime resistance provided by the ESBL plasmid.
413 This suggests epistasis between the plasmid ESBL gene and chromosomal loci that
414 vary among strains. Through comparison of the strain genomes we could not identify
415 any clear differences in chromosomal gene content among strains in terms of known
416 resistance determinants to explain the observed variation in cefotaxime resistance.
417 For example, all strains encode the same set of standard efflux pumps with the
418 exception of F047 and F048, which also contain *tetA*. Yet F047 and F048 differ
419 markedly to each other in their cefotaxime resistance response, suggesting that TetA
420 does not explain the variable resistance response. All strains encode a variant of
421 *blaEC*. In addition, F022 and F047 encode *blaTEM-1* but vary in their cefotaxime
422 resistance response, suggesting that *blaTEM-1* does not explain the variable
423 resistance response. This is perhaps unsurprising as the prediction of a strain's

424 resistance phenotype from gene content alone is notoriously inaccurate (Mahfouz et
425 al., 2020).
426
427 Comparing the transcriptomes of plasmid-carriers with their parental strain revealed
428 highly strain-specific effects of plasmid acquisition on the expression of chromosomal
429 genes. The number of genes whose transcription was affected by the plasmid was
430 small in all strains, ranging from 0 to just 22 genes (at FDR < 0.05). These data stand
431 in contrast to other studies where the expression levels of hundreds of chromosomal
432 genes are affected by plasmid acquisition (Harrison et al., 2015; Long et al., 2019;
433 Millan et al., 2015; Takahashi et al., 2015). Significant transcriptional effects of ESBL
434 plasmid acquisition were focussed in discrete operons or regulons. For example, in
435 GU15 we observed down-regulation of the sulfur biosynthesis and transport operons
436 (*cysA* – *cysW*). In F048 plasmid-carriers, flavohaemoglobin (Hmp), which is
437 responsible for resistance to nitrosative stress (Stevanin et al., 2007), was upregulated
438 following plasmid acquisition. In F047, the transcriptional impact of plasmid acquisition
439 was more widespread, affecting more diverse functions, but, consistent with F048,
440 most of these were related to stress-responses. Upregulation was observed in *marR*,
441 which did not extend to *marA*; *marA* has been demonstrated to have a short half-life
442 (3 minutes) and is quickly depleted when the environmental stress is removed (Vinué
443 et al., 2013). Increased expression was also observed in heat shock proteins IbpA/B.
444 The function of IbpA/B extends beyond heat stress; previous studies have shown that
445 increased *ibpA/B* expression resulted in the overproduction of a beta-lactamase
446 precursor, potentially through IbpA/B binding to the precursor protein, preventing
447 subsequent processing (Kuczyńska-Wiśnik et al., 2002). This could explain the
448 lowered cefotaxime MIC observed, though the exact cause of *ibpA/B* upregulation is

449 unclear. All of these factors indicate that F047 exhibited a strong stress response to
450 acquisition of the plasmid. Plasmids are known to elicit stress responses in their host
451 cells (San Millan et al., 2018), for example through the conjugation-mediated cell
452 envelope stress in *E. coli* (Yang et al., 2008). It is hypothesised the production of
453 conjugation apparatus may lead to misfolded proteins; F047 failed to conjugate in
454 shaking conditions. This may be due to an increase in the concentration of damaged
455 or misfolded proteins beyond that which would be mitigated by increased expression
456 of stress response proteins (e.g. DegP, CpxP).
457
458 In two of our strains there is evidence of a transcriptional response possibly driven by
459 the relationship between mobile genetic elements. In F022, the upregulation of
460 flagellar and chemotaxis genes was explained by a 768 bp insertion of an IS1 family
461 element encoding both *insA* and *insB* in the *lrhA* regulator. LrhA belongs to the lysR
462 family and binds to and negatively regulates expression of the *flhDC* master regulator.
463 Truncation of *lrhA* is therefore likely to have prevented negative regulation of *flhDC*,
464 leading to uncontrolled expression of the flagellar and chemotaxis operons. Genomic
465 comparison of IS elements within the F022 genome revealed 7 identical IS1
466 sequences in the parental genome, with 4 found on the chromosome, and 3 on a
467 canonical plasmid. Upon plasmid acquisition, this element inserted one additional
468 time. This appeared to be a random event, as a similar insertion could not be detected
469 in the short-read data of replicate transconjugants. In F048 a set of co-located
470 upregulated genes were associated with a chromosomal prophage. Many prophages
471 respond to host stress responses, which can be induced by plasmid acquisition and
472 thus may explain the upregulation of prophage gene expression observed here.

473 Prophages have also been shown to excise and replicate under stress conditions, but
474 we did not detect any excision or genomic amplification of the phage region.
475
476 Besides those genes whose expression was significantly altered by ESBL plasmid
477 acquisition (i.e. that met the stringent significance threshold), we also observed a
478 subtle but consistent transcriptional response to plasmid acquisition among all genes
479 with a > 2-fold change in expression. Upon acquisition of a plasmid the most intuitive
480 scenario would be a fall in chromosomal transcription as transcriptional machinery is
481 sequestered at plasmid promoters (Dunn et al., 2019). Accordingly, across all strains,
482 we observed reduction in transcription of *csg* genes encoding curli fimbriae and genes
483 involved in cell wall and outer membrane production including the *waa* LPS core
484 genes. These genes are involved in biosynthesis of energetically costly structures in
485 the cell and their repression is consistent with offsetting energetic costs of plasmid
486 maintenance. Conversely, we observed consistently increased transcription of *hya,*
487 *hyb, hyc* genes encoding the hydrogenase-1 and 3 complexes, the *nar* gene encoding
488 nitrate reductase, the *ttr* gene encoding tartrate dehydratase, and the *gad* glutamate
489 decarboxylase operon. All of these genes are involved in various aspects of anaerobic
490 metabolism, which is known to be important for colonising the mammalian gut.
491 Moreover, some of these genes exhibit negative frequency dependent selection in the
492 MDR clade C of *E. coli* ST131, which may reflect selection for enhanced intestinal
493 colonisation (McNally et al., 2019). The observation of broad-scale, subtle changes to
494 chromosomal gene expression caused by an MDR plasmid that are consistent across
495 diverse bacterial lineages warrants further investigation. Their scale is suggestive of a
496 role for plasmid-encoded regulatory elements, such as small RNAs (Vial & Hommais,
497 2020), with the potential for genome-wide effects.

498 **Conclusion**

499 We observed strain-specific but limited effects of acquisition of an ESBL plasmid
500 across diverse *E. coli* lineages. The transcriptional response to plasmid acquisition
501 was limited to differential expression of small numbers of genes within discrete
502 operons or regulons whose identity varied between strains. More subtle but consistent
503 effects of plasmid acquisition on global transcription were observed, affecting a range
504 of cellular processes. Relative growth and cefotaxime resistance of ESBL plasmid
505 carriers varied between strains. Overall, our findings suggest that the effects of MDR
506 plasmid acquisition upon the host cell arise from specific genetic interactions that are
507 likely to be difficult to predict a priori and that fitness costs are unlikely to act as a
508 barrier to plasmid transmission in natural populations of *E. coli*.

509

510 **Acknowledgements**

511 This work was funded by a BBSRC project grant [BB/R006261/1 & BB/R006253/1]
512 jointly awarded to AM and MB respectively. We would like to thank Dr. Robert Moran
513 for his feedback and guidance on pLL35.

514

515 **Figures**

516 **Figure 1 – The level of resistance to cefotaxime conferred by the pLL35 varied**
517 **by strain.** Plots are facetted by *E. coli* strain. Solid lines show the mean (n=3) ±
518 standard error of bacterial density measured using optical density (OD) at 600 nm with
519 (red) or without (blue) pLL35 across gradients of increasing cefotaxime concentration.

520

521

522 **Figure 2 – The effect of acquiring pLL35 on bacterial growth kinetics varied by**
523 **strain.** Panels show the response of the following growth parameters to plasmid
524 acquisition: (A) lag time, (B) maximum growth rate, (C) maximum density, and (D)
525 integral (i.e. area under the growth curve). Boxes show normalised values (plasmid-
526 carrying strain value divided by parental strain value) for each strain (n=5) indicating
527 the performance of plasmid carriers relative to their parental strain where a value of 1
528 represents equal performance. The lower hinge of the box denotes the 25th percentile,
529 the upper hinge denotes the 75th percentile, and the line within the box indicates the
530 median. Upper whiskers extend to the highest value no further than 1.5 times the inter-
531 quartile range from the hinge. Lower whiskers extend to the smallest value no further
532 than 1.5 times the inter-quartile range from the hinge. Points indicate outliers beyond
533 the whiskers.
534
535 **Figure 3 – Transcriptional responses to acquiring pLL35 varied by strain.** Log_2
536 fold change (CTX) of differential expression data and their statistical significance (-
537 log_{10} of the P-value). Whilst 4 of the 8 isolates showed no significant transcriptional
538 differences, other isolates showed patterns of differential expression in discrete
539 operons, or in genes under the control of a common regulator. The transcriptomic
540 effects observed in this host range are determined by strain, rather than host genetic
541 background. Blue = Significant Fold Change (>2) OR Significant P value (<0.05), Red
542 = Also FDR Significant at a threshold of <0.10, Green = Also FDR Significant at a
543 threshold of <0.05, Black = Not significant.
544
545 **Figure 4 – Transcriptional response of strain F022 was likely caused by a**
546 **chromosomal insertion of an IS element.** A) Parental genome sequence with fully

547 intact lrhA gene. B) Transconjugant genome sequence with an IS1 family transposase
548 sequence causing a truncation to lrhA. C) IS1 family transposase with left and right
549 inverted repeat sequences, and a 9 base pair target site duplication. This particular
550 IS1 occurs 7 times in the parental strain, and has inserted one additional time upon
551 plasmid conjugation. Querying the ISfinder database shows that this IS1 shares 97%
552 sequence identity with IS1 R, B and D. This element encodes two ORFs, insA and
553 insB. D) Depth of long reads uniquely mapped to the transconjugant assembly. The
554 minimum depth of reads that were successfully mapped to this region is 50, and in the
555 parental isolate there are 0 reads that map to the IS1 transposase.
556
557 **Figure 5** – Transcriptional change of genes from the extremes of the PCA distribution
558 show some common signatures of differential expression (e.g. *cit* operon, *his* operon,
559 the *hya, hyb,* and *hyc* operon, and the *nar*, *gad* and *ttd* operons). Genes were
560 extracted from the 5th and 95th percentile of the PCA distribution from figure S6 (i.e.
561 genes extraneous to the central distribution). These genes were assigned to COGS
562 functional categories, with each category ordered via UPGMA clustering of the
563 expression data.
564
565 **Supplementary Material**
566 **Figure S1** – CTX-M-15 containing plasmid pLL35. A) Genomic map of pLL35 showing
567 a complete transfer region including a full suite of conjugation machine (tra locus), and
568 a complex antibiotic resistance region that confers resistance to cephalosporins,
569 aminogylcosides and quinolones. Within this region, OXA-9 is found to contain a
570 premature stop codon. pLL35 was found to contain a novel IS element flanked by a 5
571 bp terminal site duplication (TCCTG). B) Schematic of the resistance region, which

572 contains Tn1331b that is interrupted by a 2971 bp insertion of ISEcp1 containing a
573 1315 bp passenger section that includes CTX-M-15.
574
575 **Figure S2** – Conjugational uptake of pLL35 varied with *E. coli* strain and culturing
576 conditions. Open symbols show mean ± standard error of conjugation rate for each
577 strain and culturing condition. Colour denotes culturing condition (shaken culture =
578 green; static culture = orange). Individual replicate values are shown as different
579 symbol shapes. Symbols are jittered to prevent over-plotting.
580
581 **Figure S3** – **Stable maintenance of pLL35 in all *E. coli* strains.** Plots are facetted
582 horizontally by strain. Lines show the mean (n=4) ± standard error (shaded area)
583 bacterial population densities over time from colony forming unit counts on nutrient
584 agar plates to give the whole population (blue) or nutrient agar plates supplemented
585 with 4 µg/ml of cefotaxime to give the plasmid-carrier fraction of the population (red).
586
587 **Figure S4** – **The magnitude of the transcriptional response to pLL35 acquisition**
588 **varied by strain.** A) Number of genes that were significantly (FDR <0.05) differentially
589 expressed (>2 log fold change). B) Number of genes that were significantly (FDR
590 <0.10) differentially expressed (>2 log fold change). Red = number of genes
591 upregulated, Blue = number of genes that were downregulated.
592
593 **Figure S5** – **Global transcriptional response of ~779 core genes across all**
594 **strains, sorted by functional cog category.** Gene order is determined via UPGMA
595 clustering of log2 transcriptional changes. A = Cellular processes and signalling, B =
596 Metabolism , C = Information storage and processing, D = Poorly characterised. The

597 isolates vary in their transcriptional response to the plasmid in a strain dependent
598 manner, however a large number of metabolism genes can be seen to increase in
599 transcription across all strains. Isolate F022, belonging to ST-131 Clade A -which is
600 not typically associated with MDR plasmids – exhibits the most disparate differential
601 expression profile.
602
603 **Figure S6 – PCA distributions of expression values from functionally**
604 **categorised core genes.** A = Cellular processes and signalling, B = Metabolism , C
605 = Information storage and processing. D shows how each isolate is contributing to the
606 PCA distribution. This data highlights which genes exhibit the greatest level of
607 differential expression amongst the isolates, with several candidates in each larger
608 COG category. Panel D recapitulates the phylogenetic relatedness of isolates, with
609 environmental isolates, MDR associated and non-associated lineages appearing
610 together.
611
612 **Table S1** – Accession numbers for all read data associated with this study.
613
614 **Table S2** – Variants detected in transconjugant strains and their impact on host
615 transcription, and variants detected in independent conjugation replicates. Positions
616 highlighted in bold occur in multiple replicates.
617
618

619 **References**

620 Alonso-del Valle, A., León-Sampedro, R., Rodríguez-Beltrán, J., Hernández-García,
621 M., Ruiz-Garbajosa, P., Cantón, R., San Millán, Á., Spain, M., & Peña-Miller, R.
622 (2020). The distribution of plasmid fitness effects explains plasmid persistence
623 in bacterial. In *bioRxiv*.

624 Banerjee, R., & Johnson, J. R. (2014). A New Clone Sweeps Clean: the Enigmatic
625 Emergence of Escherichia coli Sequence Type 131. *Antimicrobial Agents and*
626 *Chemotherapy*, *58*(9), 4997–5004. https://doi.org/10.1128/AAC.02824-14

627 Bouma, J. E., & Lenski, R. E. (1988). Evolution of a bacteria/plasmid association.
628 *Nature*, *335*(6188), 351–352. https://doi.org/10.1038/335351a0

629 Brockhurst, M. A., Harrison, E., Hall, J. P. J., Richards, T., McNally, A., & MacLean,
630 C. (2019). The Ecology and Evolution of Pangenomes. *Current Biology : CB*,
631 *29*(20), R1094–R1103. https://doi.org/10.1016/j.cub.2019.08.012

632 Buckner, M. M. C., Saw, H. T. H., Osagie, R. N., McNally, A., Ricci, V., Wand, M. E.,
633 Woodford, N., Ivens, A., Webber, M. A., & Piddock, L. J. V. (2018). Clinically
634 Relevant Plasmid-Host Interactions Indicate that Transcriptional and Not
635 Genomic Modifications Ameliorate Fitness Costs of Klebsiella pneumoniae
636 Carbapenemase-Carrying Plasmids. *MBio*, *9*(2).
637 https://doi.org/10.1128/mBio.02303-17

638 Chilcott, G. S., & Hughes, K. T. (2000). Coupling of flagellar gene expression to
639 flagellar assembly in Salmonella enterica serovar typhimurium and Escherichia
640 coli. *Microbiology and Molecular Biology Reviews : MMBR*, *64*(4), 694–708.
641 https://doi.org/10.1128/mmbr.64.4.694-708.2000

642 CLSI. (2012). *Methods for Dilution Antimicrobial Test for Bacteria that Grow*
643 *Aerobically. M7-A*. Wayne, PA.

644 Dunn, S. J., Connor, C., & McNally, A. (2019). The evolution and transmission of
645 multi-drug resistant Escherichia coli and Klebsiella pneumoniae: the complexity
646 of clones and plasmids. In *Current Opinion in Microbiology* (Vol. 51, pp. 51–56).
647 https://doi.org/10.1016/j.mib.2019.06.004
648 Feng, Y., Liu, L., Lin, J., Ma, K., Long, H., Wei, L., Xie, Y., McNally, A., & Zong, Z.
649 (2019). Key evolutionary events in the emergence of a globally disseminated,
650 carbapenem resistant clone in the Escherichia coli ST410 lineage.
651 *Communications Biology*, *2*, 322. https://doi.org/10.1038/s42003-019-0569-1
652 Göttig, S., Riedel-Christ, S., Saleh, A., Kempf, V. A. J., & Hamprecht, A. (2016).
653 Impact of blaNDM-1 on fitness and pathogenicity of Escherichia coli and
654 Klebsiella pneumoniae. *International Journal of Antimicrobial Agents*, *47*(6),
655 430–435. https://doi.org/10.1016/j.ijantimicag.2016.02.019
656 Harrison, E., Guymer, D., Spiers, A. J., Paterson, S., & Brockhurst, M. A. (2015).
657 Parallel Compensatory Evolution Stabilizes Plasmids across the Parasitism-
658 Mutualism Continuum. *Current Biology*, *25*(15), 2034–2039.
659 https://doi.org/10.1016/j.cub.2015.06.024
660 Kottara, A., Hall, J. P. J., Harrison, E., & Brockhurst, M. A. (2018). Variable plasmid
661 fitness effects and mobile genetic element dynamics across Pseudomonas
662 species. *FEMS Microbiology Ecology*, *94*(1), 172.
663 https://doi.org/10.1093/femsec/fix172
664 Kuczyńska-Wiśnik, D., Kędzierska, S., Matuszewska, E., Lund, P., Taylor, A.,
665 Lipińska, B., & Laskowska, E. (2002). The Escherichia coli small heat-shock
666 proteins IbpA and IbpB prevent the aggregation of endogenous proteins
667 denatured in vivo during extreme heat shock. *Microbiology*.
668 https://doi.org/10.1099/00221287-148-6-1757

669 Long, D., Zhu, L. L., Du, F. L., Xiang, T. X., Wan, L. G., Wei, D. D., Zhang, W., & Liu,
670 Y. (2019). Phenotypical profile and global transcriptomic profile of Hypervirulent
671 Klebsiella pneumoniae due to carbapenemase-encoding plasmid acquisition.
672 *BMC Genomics*, *20*(1), 480. https://doi.org/10.1186/s12864-019-5705-2
673 Mahfouz, N., Ferreira, I., Beisken, S., von Haeseler, A., & Posch, A. E. (2020).
674 Large-scale assessment of antimicrobial resistance marker databases for
675 genetic phenotype prediction: a systematic review. *Journal of Antimicrobial*
676 *Chemotherapy*. https://doi.org/10.1093/jac/dkaa257
677 Mathers, A. J., Peirano, G., & Pitout, J. D. D. (2015). The role of epidemic resistance
678 plasmids and international high-risk clones in the spread of multidrug-resistant
679 Enterobacteriaceae. *Clinical Microbiology Reviews*, *28*(3), 565–591.
680 https://doi.org/10.1128/CMR.00116-14
681 McNally, A., Kallonen, T., Connor, C., Abudahab, K., Aanensen, D. M., Horner, C.,
682 Peacock, S. J., Parkhill, J., Croucher, N. J., & Corander, J. (2019).
683 Diversification of Colonization Factors in a Multidrug-Resistant Escherichia coli
684 Lineage Evolving under Negative Frequency-Dependent Selection. *MBio*, *10*(2).
685 https://doi.org/10.1128/mBio.00644-19
686 McNally, A., Oren, Y., Kelly, D., Pascoe, B., Dunn, S., Sreecharan, T., Vehkala, M.,
687 Välimäki, N., Prentice, M. B., Ashour, A., Avram, O., Pupko, T., Dobrindt, U.,
688 Literak, I., Guenther, S., Schaufler, K., Wieler, L. H., Zhiyong, Z., Sheppard, S.
689 K., … Corander, J. (2016). Combined Analysis of Variation in Core, Accessory
690 and Regulatory Genome Regions Provides a Super-Resolution View into the
691 Evolution of Bacterial Populations. *PLoS Genetics*, *12*(9), e1006280.
692 https://doi.org/10.1371/journal.pgen.1006280
693 Millan, A. S., Toll-Riera, M., Qi, Q., & MacLean, R. C. (2015). Interactions between

694 horizontally acquired genes create a fitness cost in Pseudomonas aeruginosa.
695 *Nature Communications*, *6*. https://doi.org/10.1038/ncomms7845
696 Nang, S. C., Morris, F. C., McDonald, M. J., Han, M. L., Wang, J., Strugnell, R. A.,
697 Velkov, T., & Li, J. (2018). Fitness cost of mcr-1-mediated polymyxin resistance
698 in Klebsiella pneumoniae. *Journal of Antimicrobial Chemotherapy*, *73*(6), 1604–
699 1610. https://doi.org/10.1093/jac/dky061
700 Peirano, G., Schreckenberger, P. C., & Pitout, J. D. D. (2011). Characteristics of
701 NDM-1-Producing Escherichia coli Isolates That Belong to the Successful and
702 Virulent Clone ST131. *Antimicrobial Agents and Chemotherapy*, *55*(6), 2986–
703 2988.
704 Petty, N. K., Zakour, N. L. Ben, Stanton-Cook, M., Skippington, E., Totsika, M.,
705 Forde, B. M., Phan, M. D., Moriel, D. G., Peters, K. M., Davies, M., Rogers, B.
706 A., Dougan, G., Rodriguez-Baño, J., Pascual, A., Pitout, J. D., Upton, M.,
707 Paterson, D. L., Walsh, T. R., Schembri, M. A., & Beatson, S. A. (2014). Global
708 dissemination of a multidrug resistant Escherichia coli clone. *Proc Natl Acad Sci*
709 *U S A*, *doi/10.107*.
710 San Millan, A., Toll-Riera, M., Qi, Q., Betts, A., Hopkinson, R. J., McCullagh, J., &
711 MacLean, R. C. (2018). Integrative analysis of fitness and metabolic effects of
712 plasmids in Pseudomonas aeruginosa PAO1. *The ISME Journal*, *12*(12), 3014–
713 3024. https://doi.org/10.1038/s41396-018-0224-8
714 Seemann, T. (2014). Prokka: rapid prokaryotic genome annotation. *Bioinformatics*,
715 *30*(14), 2068–2069. https://doi.org/10.1093/bioinformatics/btu153
716 Stevanin, T. M., Read, R. C., & Poole, R. K. (2007). The hmp gene encoding the
717 NO-inducible flavohaemoglobin in Escherichia coli confers a protective
718 advantage in resisting killing within macrophages, but not in vitro: Links with

719 swarming motility. *Gene*, *398*(1-2 SPEC. ISS.), 62–68.
720 https://doi.org/10.1016/j.gene.2007.03.021
721 Takahashi, Y., Shintani, M., Takase, N., Kazo, Y., Kawamura, F., Hara, H., Nishida,
722 H., Okada, K., Yamane, H., & Nojiri, H. (2015). Modulation of primary cell
723 function of host Pseudomonas bacteria by the conjugative plasmid pCAR1.
724 *Environmental Microbiology*, *17*(1), 134–155. https://doi.org/10.1111/1462-
725 2920.12515
726 Vial, L., & Hommais, F. (2020). Plasmid-chromosome cross-talks. *Environmental*
727 *Microbiology*, *22*(2), 540–556. https://doi.org/10.1111/1462-2920.14880
728 Vinué, L., Mcmurry, L. M., & Levy, S. B. (2013). The 216-bp marB gene of the
729 marRAB operon in Escherichia coli encodes a periplasmic protein which
730 reduces the transcription rate of marA. *FEMS Microbiology Letters*.
731 https://doi.org/10.1111/1574-6968.12182
732 Wick, R. R., Judd, L. M., Gorrie, C. L., & Holt, K. E. (2017). Unicycler: Resolving
733 bacterial genome assemblies from short and long sequencing reads. *PLoS*
734 *Computational Biology*, *13*(6), e1005595.
735 https://doi.org/10.1371/journal.pcbi.1005595
736 Wright, R. C. T., Friman, V.-P., Smith, M. C. M., & Brockhurst, M. A. (2018). Cross-
737 resistance is modular in bacteria-phage interactions. *PLoS Biology*, *16*(10),
738 e2006057. https://doi.org/10.1371/journal.pbio.2006057
739 Wu, W., Feng, Y., Tang, G., Qiao, F., McNally, A., & Zong, Z. (2019). NDM Metallo-
740 beta-Lactamases and Their Bacterial Producers in Health Care Settings. *Clinical*
741 *Microbiology Reviews*, *32*(2). https://doi.org/10.1128/CMR.00115-18
742 Yang, X., Ma, Q., & Wood, T. K. (2008). The R1 conjugative plasmid increases
743 Escherichia coli biofilm formation through an envelope stress response. *Applied*

and Environmental Microbiology, *74*(9), 2690–2699. https://doi.org/10.1128/AEM.02809-07

Zong, Z., Fenn, S., Connor, C., Feng, Y., & McNally, A. (2018). Complete genomic characterization of two Escherichia coli lineages responsible for a cluster of carbapenem-resistant infections in a Chinese hospital. *Journal of Antimicrobial Chemotherapy*, *73*(9), 2340–2346. https://doi.org/10.1093/jac/dky210

751

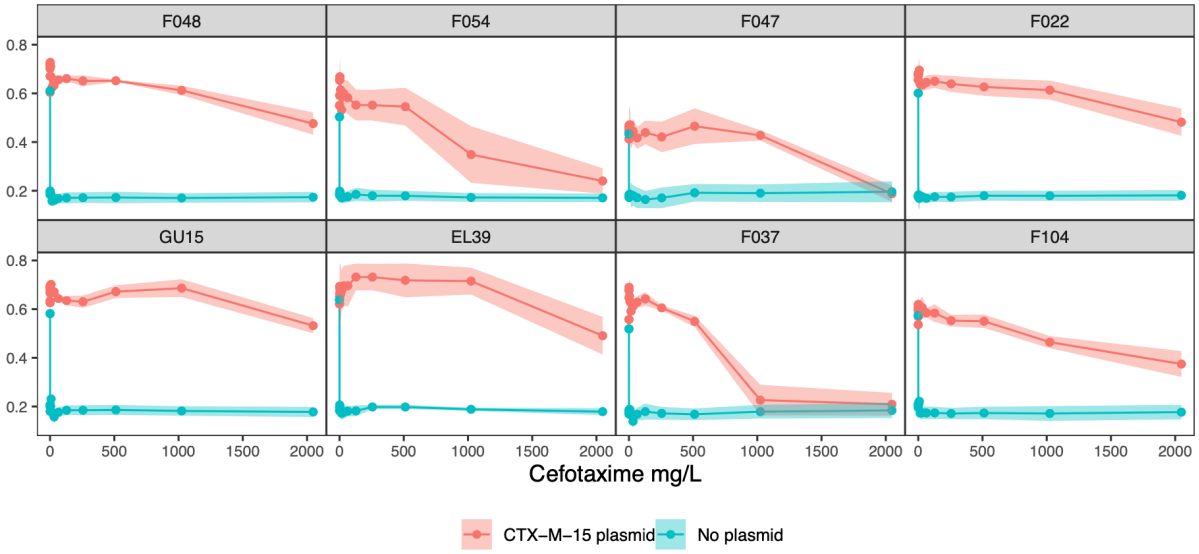
F048
F054
F047
F022
GU15
EL39
F037
F104
0.8
0.6
0.4
0.2
0
500
1000
1500
2000
Cefotaxime mg/L
CTX−M−15 plasmid
No plasmid

752

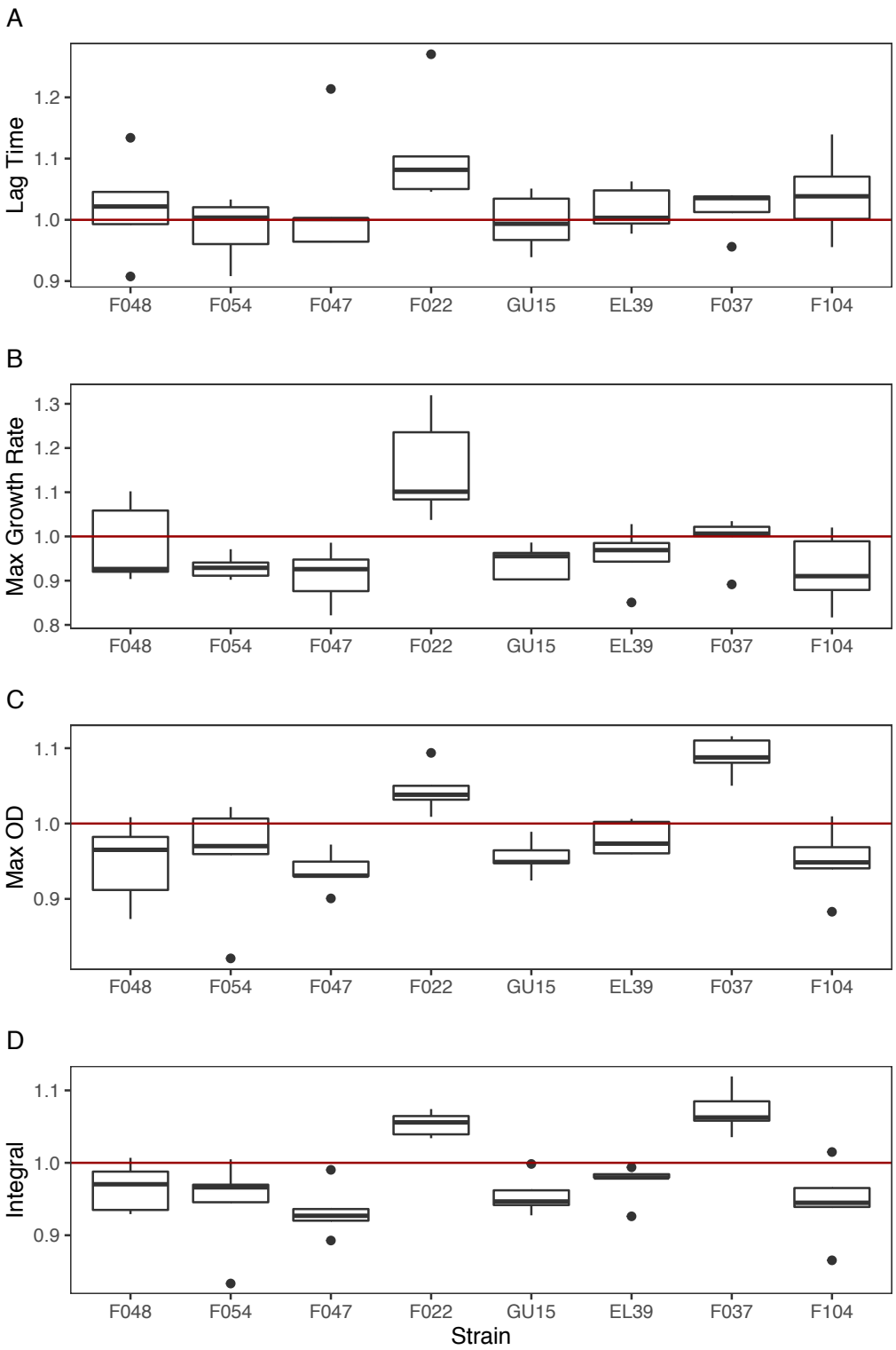
A
Lag Time
1.2
1.1
1.0
0.9
F048
F054
F047
F022
GU15
EL39
F037
F104
B
Max Growth Rate
1.3
1.2
1.1
1.0
0.9
0.8
F048
F054
F047
F022
GU15
EL39
F037
F104
C
Max OD
1.1
1.0
0.9
F048
F054
F047
F022
GU15
EL39
F037
F104
D
Integral
1.1
1.0
0.9
F048
F054
F047
F022
GU15
EL39
F037
F104
Strain

753

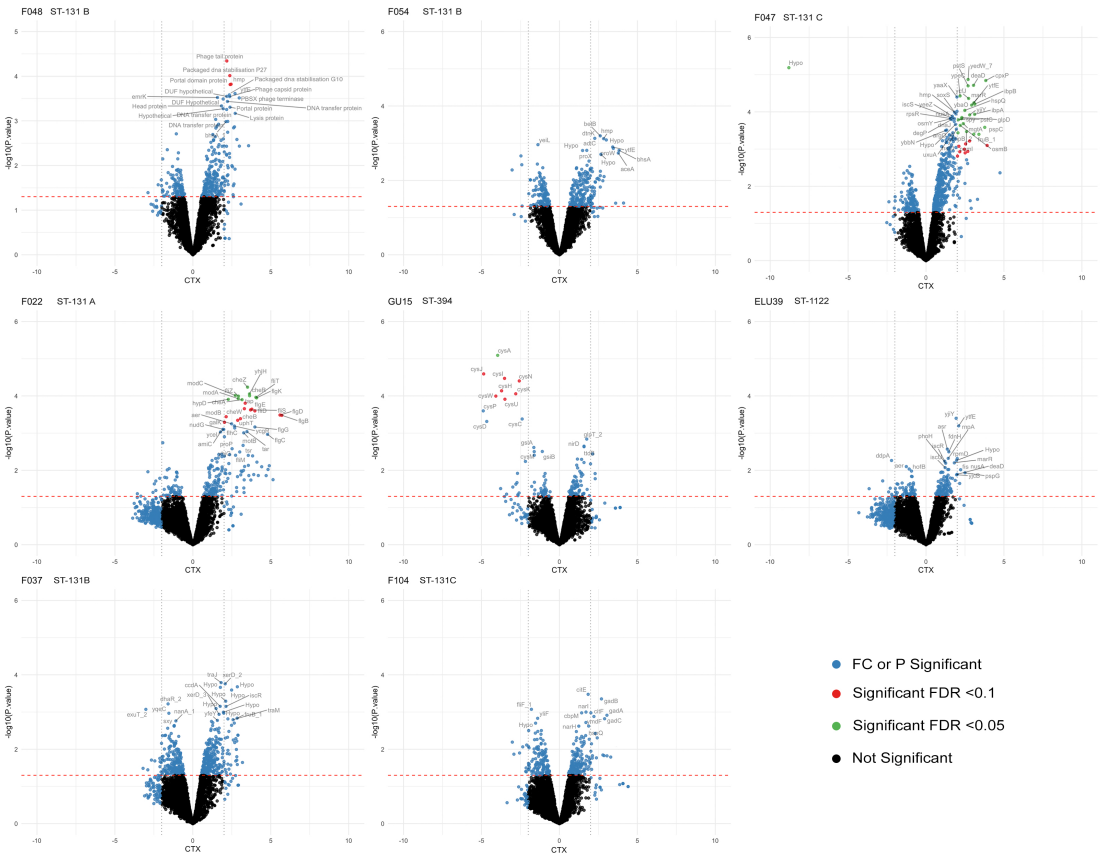
F048 ST-131 B
F054 ST-131 B
F047 ST-131 C
F022 ST-131 A
GU15 ST-394
ELU39 ST-1122
F037 ST-131B
F104 ST-131C
-log10(P-value)
CTX
FC or P Significant
Significant FDR <0.1
Significant FDR <0.05
Not Significant

754

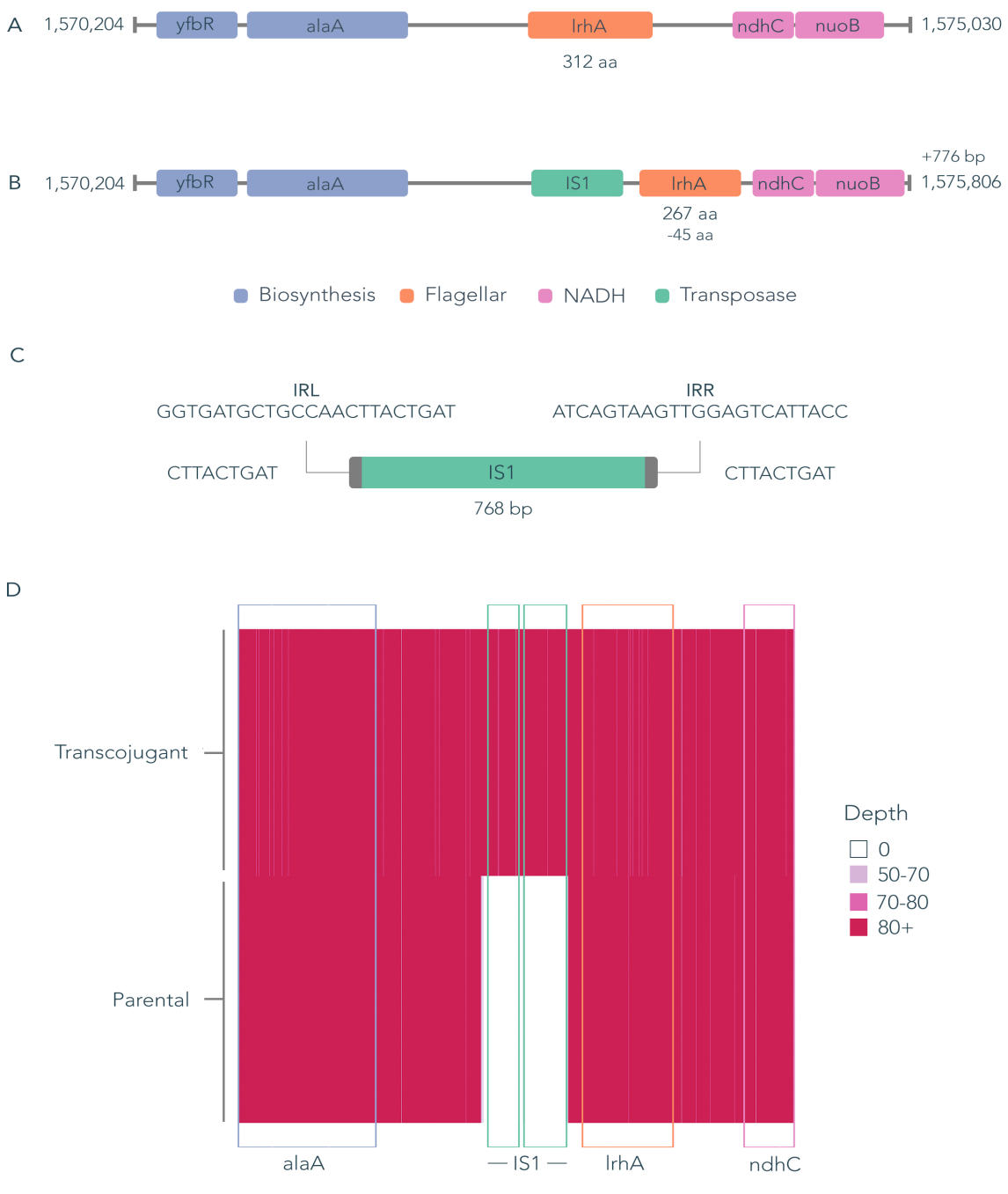
A
1,570,204
yfbR
alaA
lrhA
ndhC
nuoB
1,575,030
312 aa
B
1,570,204
yfbR
alaA
IS1
lrhA
ndhC
nuoB
+776 bp
1,575,806
267 aa
-45 aa
Biosynthesis
Flagellar
NADH
Transposase
C
IRL
GGTGATGCTGCCAACTTACTGAT
IRR
ATCAGTAAGTTGGAGTCATTACC
CTTACTGAT
IS1
CTTACTGAT
768 bp
D
Transcojugant
Parental
Depth
0
50-70
70-80
80+
alaA
IS1
lrhA
ndhC

755

Cellular Processes and Signalling
Information Storage and Processing
Metabolism
Poorly Characterised
wzxC
clpB
dnaK
hspQ
ibpB
ibpA
pspD
asr
phoH
ytfE
cpxP
hycH
tsr
hofQ
ytcA
sdsP
tar
yhjH
tap
yeaY
yegQ
ybjH
nrdH
rpoD
soxS
ybaQ
marR
deaD
rplF
rplC
rplD
nusA
rpsR
pspA
pspC
yiiE
uvrA
hslR
malE
phnL
ssuA
hycF
ydiN
livM
ybbW
lysK
narG
hmp
corA
mqtA
iscU
iscS
nirD
metK
narJ
narH
gadB
gadC
gadA
rhaA
uacT
ygcQ
rhaD
eutT
phnM
eutA
phnI
yhfS
ydjJ
xylF
dppC
frwC
rhaB
cmtA
yihU
thiH
rhaT
yphF
fixC
yjcS
ptsA
sgbH
eutD
ssnA
eutJ
eutG
phnK
yphD
yhfW
phnE
phnG
cysJ
cysP
cusF
nudI
gsiD
glnK
psuK
psuG
ydhC
pstA
pstC
pstS
nrdI
narI
fruK
yiiG
pspG
ybhH
ygcW
pliG
yjbG
iscA
pspB
yoeB
ybiJ
yjcB
yaaH
ygbA
yhiM
Gene Expression (fold change log2)
Up (5)
Down (-5)
Isolate: F048 F054 F047 F022 GU15 EL39 F037 F104
Sequence Type: 131-B 131-B 131C 131-A 394 1122 131-B 131-C
Phylogroup: B2 B2 B2 B2 D A B2 B2
UPGMA Clustering: